

Observations of acoustic surface waves in outdoor sound propagation

Donald G. Albert^{a)}

U.S. Army Cold Regions Research and Engineering Laboratory, 72 Lyme Road, Hanover, New Hampshire 03755-1290

(Received 8 October 2001; revised 6 January 2003; accepted 17 January 2003)

Acoustic surface waves have been detected propagating outdoors under natural conditions. Two critical experimental conditions were employed to ensure the conclusive detection of these waves. First, acoustic pulses rather than a continuous wave source allowed an examination of the waveform shape and avoided the masking of wave arrivals. Second, a snow cover provided favorable ground impedance conditions for surface waves to exist. The acoustic pulses were generated by blank pistol shots fired 1 m above the snow. The resultant waveforms were measured using a vertical array of six microphones located 60 m away from the source at heights between 0.1 and 4.75 m. A strong, low frequency “tail” following the initial arrival was recorded near the snow surface. This tail, and its exponential decay with height (z) above the surface ($\sim e^{-\alpha z}$), are diagnostic features of surface waves. The measured attenuation coefficient α was 0.28 m^{-1} . The identification of the surface wave is confirmed by comparing the measured waveforms with waveforms predicted by the theoretical evaluation of the explicit surface wave pole term using residue theory. © 2003 Acoustical Society of America. [DOI: 10.1121/1.1559191]

PACS numbers: 43.28.En, 43.28.Fp, 43.35.Pt [LCS]

I. INTRODUCTION

In this paper experimental evidence confirming the existence of acoustic surface waves in a natural, outdoor setting is presented. Such waves require the proper ground surface impedance conditions to exist. While acoustic surface waves have been discussed for a long time in the literature, they have not been unequivocally observed in outdoor propagation experiments. Theory¹⁻⁴ predicts that these waves propagate horizontally near the ground at a phase velocity less than the velocity of sound in the air and decay exponentially with height above the surface. Laboratory measurements over hard-backed layers of felt or specially constructed model surfaces have detected these waves using both continuous and pulse sources.^{3,5-16} A few outdoor experiments have revealed an increase in the received energy at low frequencies (greater than the 6 dB level expected from a rigid boundary),^{3,17} but others have not detected such waves,¹⁸ nor have they been observed in outdoor measurements over grass using pulses.¹⁹⁻²¹ Raspet and Baird²² give a convincing theoretical argument for their existence and Daigle *et al.*¹⁴ present very clear evidence from indoor pulse experiments.

Theoretically, acoustic surface waves will exist when the imaginary part of the ground impedance exceeds the real part; this condition is expected for porous ground layers with a rigid backing. For outdoor experiments, one of the most favorable situations for acoustic surface waves is a thin layer of snow over frozen ground.^{23,24} In this paper experiments that were conducted to search for surface waves under these favorable ground impedance conditions are discussed. The measured waves show the predicted exponential decay with height above the ground surface and the observed waveforms

agree with those predicted by the theoretical evaluation of the surface wave pole using residue theory.

II. THEORY

The interaction of a spherical wave from a point source with a plane boundary is a classical problem in electromagnetics, acoustics, and seismology.²⁵⁻²⁸ For a velocity potential ϕ , the analysis starts with the Sommerfeld representation of a monofrequency spherical wave as a sum of cylindrical waves,²⁵

$$\phi = \frac{A e^{ikr}}{r} = A \int_0^\infty \frac{e^{-\gamma|z|}}{\gamma} J_0(kr) k dk, \quad (1)$$

with J_0 the Bessel function of the first kind and zeroth order, k the radial wavenumber, z the depth coordinate, r the slant distance to the observation point, and

$$i\gamma = (k_0^2 - k^2)^{1/2}, \quad \text{Re}(\gamma) > 0.$$

A coordinate transformation $k = k_0 \sin \theta$, where θ is complex^{2,25} and $k_0 = \omega/c_0$ is the wavenumber in air, converts the integral in Eq. (1) into a contour integral. By substituting Hankel functions for the Bessel function and by using approximations for large kr , the reflected wave potential can be written as^{2,21,25,29}

$$\begin{aligned} \phi^{\text{refl}} = & A \left(\frac{k_0}{2\pi r} \right)^{1/2} e^{i\pi/4} \int_{-\pi/2+i\infty}^{-\pi/2-i\infty} e^{ik_0 r_2 \cos(\theta-\theta_0)} \\ & \times R_p(\theta) \sqrt{\sin \theta} d\theta, \end{aligned} \quad (2)$$

where $R_p(\theta)$ is the plane wave reflection coefficient for angle of incidence θ and r_2 is the reflected ray path length (see Fig. 1). The integral can be evaluated by deforming the

^{a)}Electronic mail: dalbert@crrel.usace.army.mil

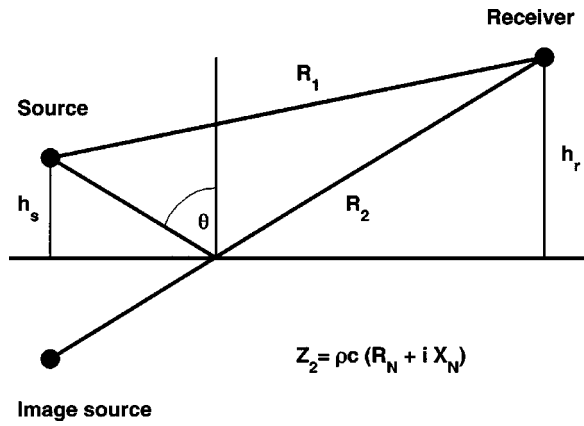


FIG. 1. Sketch of the geometry. The source and receiver are located in a homogeneous atmosphere above a plane ground surface with impedance Z_2 .

contour to the steepest descent path, leading to an expression,^{30–32}

$$\phi^{\text{refl}} = A \frac{e^{ik_0 r_2}}{r_2} [R_p + (1 - R_p)F(w)], \quad (3)$$

where $F(w)$ is called the boundary loss factor and w is a numerical distance. The acoustic surface wave is not derived as a separate term in this approach, but if it exists [see Eq. (7) below] it is included in $F(w)$. With the addition of the direct wave term $A e^{ik_0 r_1}/k_0 r_1$ where r_1 is the slant distance for the direct wave, the “full waveform” expression for the potential is obtained:

$$\frac{\phi}{A} = \frac{e^{ik_0 r_1}}{r_1} + \frac{e^{ik_0 r_2}}{r_2} [R_p + (1 - R_p)F(w)]. \quad (4)$$

The integrand of Eq. (2) has a pole where the denominator of the plane wave reflection coefficient,

$$R_p(\theta) = \frac{Z_2 \cos \theta - \rho c}{Z_2 \cos \theta + \rho c}, \quad (5)$$

is zero. Here $Z_2 = R + iX = \rho c (R_N + iX_N)$ is the characteristic specific impedance of the ground with normalized components R_N and X_N and a locally reacting ground surface has been assumed. The pole will give a contribution to the integral equation (2) when the deformation of the original contour to the steepest descent path crosses this pole; at grazing incidence this leads to the condition²

$$\left| \frac{X_N}{R_N} \right| \geq \left(1 + \frac{R_N^2}{(R_N^2 + X_N^2)^2} \right)^{-1/2}, \quad (6)$$

i.e., the surface wave exists when

$$\text{Im}(Z_2) \geq \text{Re}(Z_2). \quad (7)$$

Thus highly absorbing grounds will provide favorable conditions for acoustic surface waves to be observed. The contribution from the surface wave pole to the reflected pressure can be evaluated using residue theory to obtain^{29,33}

$$\phi^{\text{surf}} = -A \frac{k_0 \beta}{2} e^{-ik_0 h \beta} H_0^{(1)} [k_0 r_2 (1 - \beta^2)^{1/2}], \quad (8)$$

where $H_0^{(1)}$ is the Hankel function of the first kind, $\beta = \rho c / Z_2$ and $h = h_s + h_r$ is the sum of the source and receiver

heights. Donato² has shown that the theoretical surface wave phase velocity is

$$v = c \frac{X_N}{(1 + X_N^2)^{1/2}}, \quad (9)$$

and the vertical attenuation is

$$\alpha = k_0 \frac{X_N}{X_N^2 + R_N^2}. \quad (10)$$

The horizontal attenuation is the same as the decay in $H_0^{(1)} \sim r^{-1/2}$.

The acoustic pressure is related to the velocity potential by

$$P = -\rho_0 \frac{\partial \phi}{\partial t} = -i \rho_0 \omega \phi = \frac{P_0}{k_0 r} e^{i(k_0 r - \omega t)},$$

with

$$P_0 = -i \rho_0 \omega k_0 A$$

representing the source strength in Pascals, and $-i$ representing a phase shift. Then the full waveform expression, Eq. (4), becomes

$$\frac{P}{P_0} = \frac{e^{ik_0 r_1}}{k_0 r_1} + \frac{e^{ik_0 r_2}}{k_0 r_2} [R_p + (1 - R_p)F(w)], \quad (11)$$

and the explicit expression for the surface wave pressure is

$$\frac{P^{\text{surf}}}{P_0} = -\frac{\beta}{2} e^{-ik_0 h \beta} H_0^{(1)} [k_0 r_2 (1 - \beta^2)^{1/2}]. \quad (12)$$

III. EXPERIMENTAL MEASUREMENTS

A. Method

Experiments were designed to detect and identify surface waves by their chief property: their amplitude decay as a function of height above the ground surface. A microphone array was installed at an undisturbed site in Hanover, NH to obtain waveform measurements as a function of distance and height under various ground conditions, including grass, frozen ground, and various snow layers during the course of a winter. An impulsive source was selected so that the waveform characteristics could be used to identify all of the wave arrivals, rather than just recording the overall sound levels as for measurements using continuous wave sources.

The acoustic source was a .45 caliber blank pistol held at a height of 1 m and pointed toward the sensor array. A vertical array of Globe Model 100C low frequency microphones installed on a wooden tower 60 m away from the source were used as receivers. These microphones were positioned at heights of 0.5, 1, 1.5, 2, 3, and 4.75 m above the soil surface. A surface microphone (0.1 m high) also was placed at the ground or on the snow surface next to the tower just before the measurements were made (Fig. 2). The received waveforms were recorded using a Bison Model 9048 digital seismograph at a 5-kHz rate. The bandwidth of the instruments is 3 Hz to 2 kHz, but the overall bandwidth of the measurements is limited by the source output and is estimated as 5–500 Hz.

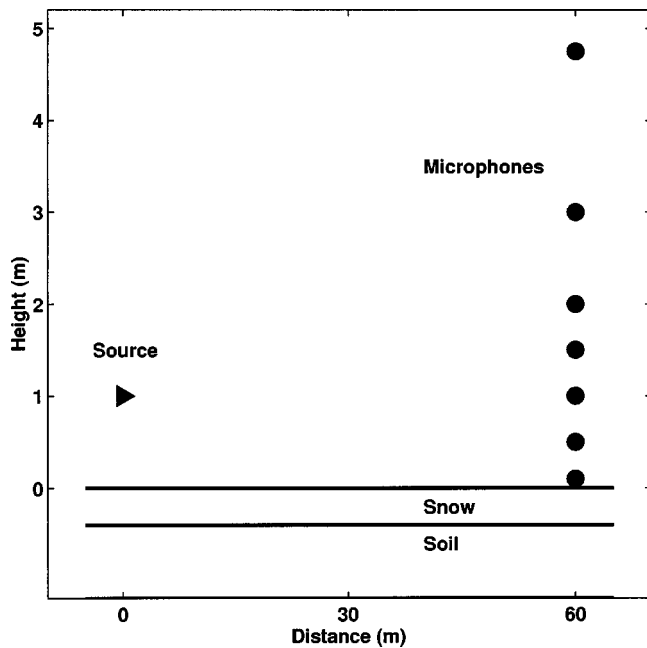


FIG. 2. Sketch of the experimental measurement geometry. The source (triangle) was a pistol firing blanks towards the microphones (circles), which were located 60 m away at heights of 0.1 m above the soil or snow surface, and 0.5, 1, 1.5, 2, 3, and 4.75 m above the soil surface. With this geometry, the grazing angle for the specularly reflected wave varied from less than 1° to 4.8° . (This sketch is not to scale, and the snow cover thickness is greatly exaggerated.)

The snow and frost depths and the snow stratigraphy, temperature, density, grain size, and crystal type were determined for each snow layer present. Meteorological data were collected using a Campbell Scientific Model 21X data logger. Temperatures were measured within the ground and snow and at various heights up to 5 m in the air. Wind speeds and directions were also recorded, along with relative humidity and barometric pressure.

B. Observations

Figure 3 shows the waveforms recorded by the tower microphones for one of the eight shots recorded on each of six separate occasions, in chronological order from left to right. In columns 1 and 2, the waveforms were recorded over cold, dry, continuous snow covers. The waveforms in columns 3 and 4 were recorded over wet, ripe snowpacks, with the snow cover for Experiment 4 nonuniform in depth because the snowmelt had begun. The waveforms in columns 5 and 6 were recorded over bare frozen ground and unfrozen grassland, respectively. The snow cover and ground characteristics for these measurements are given in Table I. The waveforms recorded without snow present (columns 5 and 6) show virtually no change in shape as a function of receiver height above the surface. Those recorded over snow show an initial pulse followed by a low frequency “tail” that decreases in amplitude with microphone height above the surface. This tail is identified as the acoustic surface wave. The acoustic surface wave is especially clear in the waveforms recorded during Experiment 2, over a 0.21-m-thick snow cover, so this particular experiment will be examined in the rest of this paper.

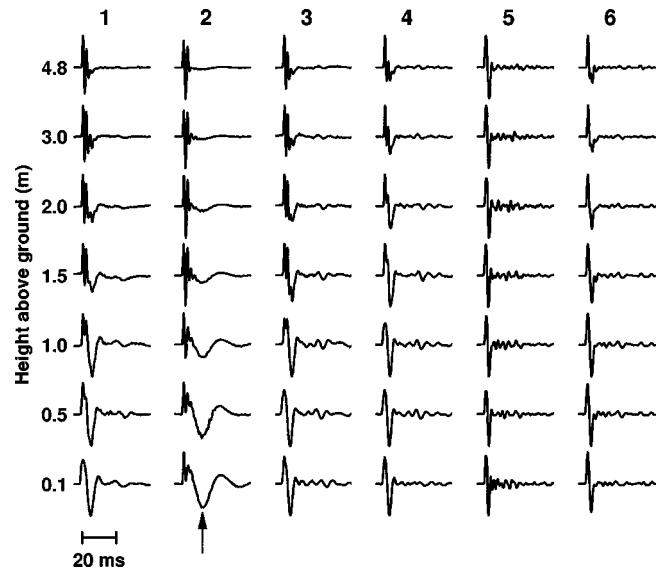


FIG. 3. Normalized low frequency microphone waveforms recorded at a 60 m range and various heights from a .45 caliber pistol shot 1 m high above the snow or ground surface. These waveforms were recorded with the same microphone array on six separate days. An arrow points to the “tail” identified as the surface wave; it is present only when snow was on the ground. Experiment numbers at the top of the columns refer to the parameters listed in Table I. Experiments 1 and 2 were conducted over dry snow covers, 3 over a wet, ripe snow cover, 4 over discontinuous wet snow, 5 over bare frozen ground, and 6 over grass. The surface wave is present in Experiments 1–4, but is strongest over the dry snow cover in Experiment 2. This case will be analyzed in the rest of the paper.

Figure 4 shows a semilogarithmic plot of the surface wave amplitude as a function of height for the eight shots recorded during Experiment 2. The absolute value of the amplitude of the negative portion of the surface wave (marked with an arrow in Fig. 3) is plotted, as these amplitudes were easy to determine without interference from the initial impulse. These values fall on a nearly straight line,

$$P(z) = P_0(r) e^{-\alpha z}, \quad (13)$$

as expected for an exponential decay where α is the decay coefficient and z the height. The slope obtained by a least squares fit (shown as a dashed line in the figure) to the lower microphones gives $\alpha = 0.28 \pm 0.1 \text{ m}^{-1}$.

Some of the deviation of the amplitudes shown in Fig. 4 from a straight line is likely to be caused by differences in microphone sensitivity. Attempts were made to calibrate the Globe microphones using a pistonphone, but difficulty in coupling the pistonphone consistently to the microphones using a special adapter made this procedure questionable, so the manufacturer’s sensitivity values have been used. The figure also shows that the amplitude values for a given microphone were very consistent, indicating that the blank pistol output was also consistent from shot to shot. The microphone sensitivity differences will not affect the analysis based on waveform shape.

IV. COMPARISON WITH THEORY

To compare the measurements with theoretical predictions, a waveform inversion procedure³⁴ was used to derive the acoustic parameters of the snow or soil. In this method,

TABLE I. Snow cover and ground parameters for the experimental measurements shown in Fig. 3.

Experiment number	Description	Effective flow resistivity σ (kN s m^{-4})	Snow depth (cm)	Porosity Ω	Density (kg m^{-3})
1	Dry snow, flat grains	55	5	0.89	100
2	Dry snow, spherical grains	11	21	0.81	170
3	Wet ripe snow	59	5	0.68	290
4	Patchy wet snow	140	3	0.74	240
5	Frozen ground	1400	-	0.34	1600
6	Grass	300	-	0.34	1600
	Lower half space (frozen soil)	3000	-	0.27	1750

Attenborough's rigid porous, layered model of ground impedance^{35,36} is used to calculate theoretical waveforms for the surface microphone using the full waveform expression, Eq. (11), above. The model parameters were varied using a simplex search algorithm until good agreement was obtained between the theoretical and the observed waveforms. Albert³⁴ has shown that for the low frequencies and short propagation ranges used in these experiments, a unique solution is obtained and both the meteorological conditions and the details of the snow layering are relatively unimportant. Since the acoustic wavelengths range from about 0.75 m at 400 Hz to 7.5 m at 40 Hz, sufficient accuracy is obtained by considering the snow to be a single layer on top of a frozen soil halfspace. The acoustic parameters determined by the waveform inversion method are listed in Table I.

Using this method of waveform inversion to determine the ground impedance was critical to the success in accurately modeling the acoustic surface waves. Although a for-

ward modeling approach (guessing the snow parameters used to calculate the waveforms) was able to predict the general behavior of the waves,³⁷ the theoretical waveforms did not match the measured waveforms very well until this inversion method was used to accurately determine the snow parameters. This sensitivity of the waveforms to the ground impedance parameters also has been noted by Daigle and co-workers.¹⁴

Once the acoustic snow cover parameters were obtained by matching the observed waveforms at the surface, theoretical waveforms were calculated at the remaining measurement heights. Figure 5 compares the measured and theoretical waveforms for all of the microphone heights for Experiment 2. The waveforms agree well not only for the surface microphone, where the inversion procedure was used to derive the snow parameters, but also for all of the microphones at different heights, showing that the full waveform solution correctly predicts the surface wave decay with height. The the-

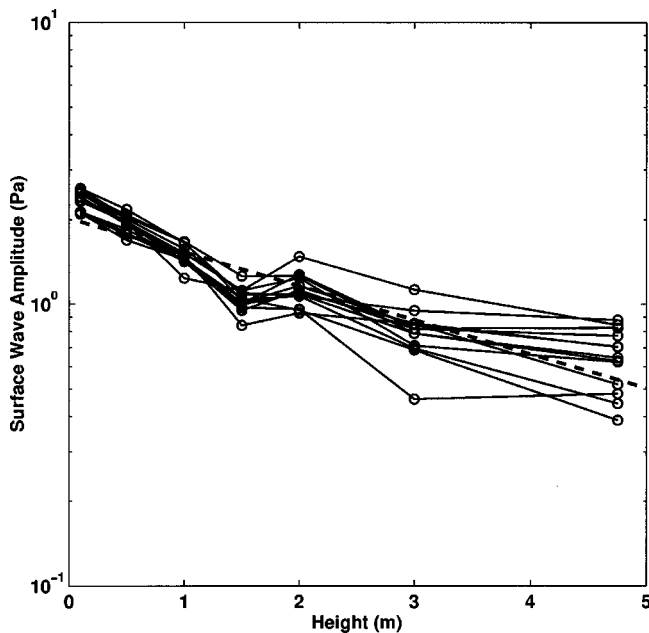


FIG. 4. Amplitude of the negative portion of the surface waveform as a function of height for eight shots recorded during Experiment 2 with a 0.21-m-thick snow cover present. A least squares fit of the measurements is shown by a dashed line and gives a decay constant of $\alpha = 0.28 \pm 0.1 \text{ m}^{-1}$.

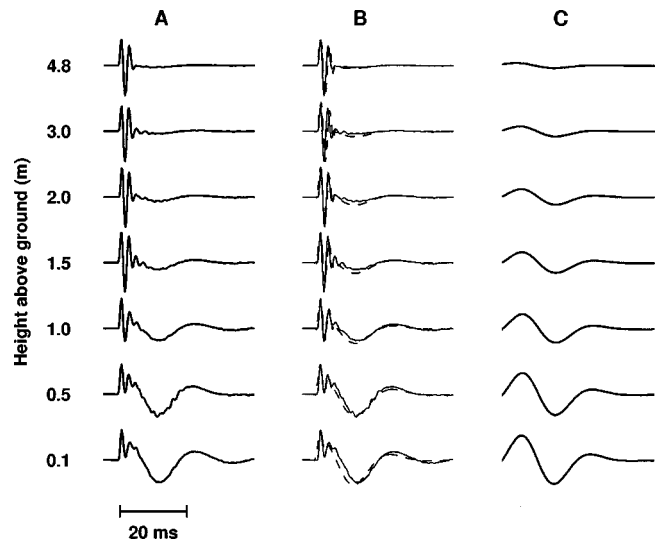


FIG. 5. A comparison between normalized measured and theoretical waveforms at a 60 m range for Experiment 2 with a 0.21-m-thick snow cover present on the ground. The parameters used in these calculations are given in Table I. Column (A) The measured waveforms as a function of height. Column (B) Overlay of the measured (solid lines) and theoretical (dashed lines) waveforms calculated using Eq. (11). Column (C) Theoretical surface wave term calculated using Eq. (12), and plotted at the same amplitude as the theoretical waveforms in Column (B).

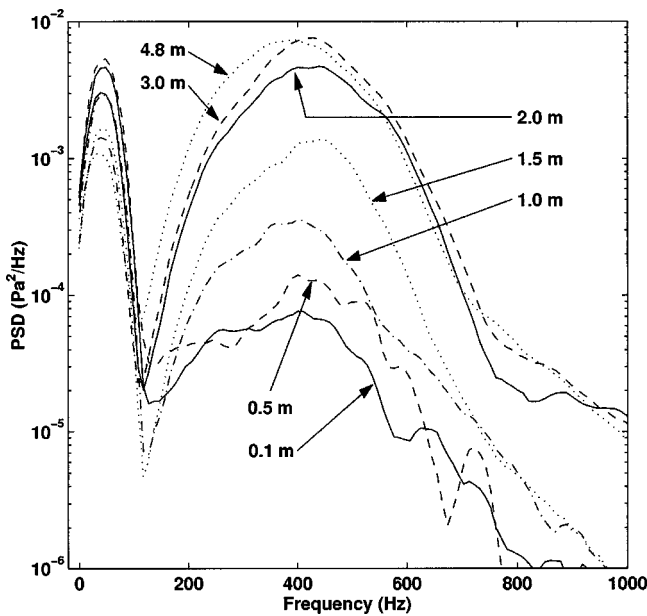


FIG. 6. Power spectral densities calculated from the measured waveforms for Experiment 2. The solid, dashed, dot-dashed, and dotted lines are the spectra for microphones at heights of 0.1, 0.5, 1, and 1.5 m, respectively. These spectra are the largest at 40 Hz and the smallest at 400 Hz. The remaining solid, dashed, and dotted lines are the spectra for microphones at 2, 3, and 4.75 m.

oretical surface wave pulses determined using Eq. (12) are also shown in the figure. These waveforms match the shape and decay with height of the observed surface wave “tail,” conclusively confirming the identification of this waveform as an acoustic surface wave. The theoretical waveforms also exhibit noncausal behavior; the pressure waveform begins slightly before the direct wave arrival. This noncausal behavior is commonly observed in surface wave calculations in seismology, and arises because terms which would cancel out the early arrivals in the full waveform calculation have been neglected in the approximate surface wave expression given by Eq. (12). Nevertheless, the agreement between the measured data and the theoretical surface wave pulse from Eq. (12) is strong evidence that the acoustic surface wave has been correctly identified in the measurements.

Figure 6 shows the frequency content of the measured waveforms for Experiment 2. The calculations used the multiple window method of Thomson.³⁸ The peak at 42 Hz is attributed to the surface wave, and agrees approximately with the period of the waveform for the microphone at the surface (about 25 ms). As shown in Fig. 7, the spectral amplitude at this frequency decreases as the microphone height increases, and this decrease agrees with the trend determined for the surface wave in the time domain shown in Fig. 4. At 400 Hz, the largest spectral amplitudes occur for the higher microphones. These spectra show that high frequencies are attenuated and low frequencies enhanced for microphones close to the snow cover surface (Fig. 4 of Ref. 39).

The acoustic surface impedance predicted using Attenborough’s model for Experiment 2 is shown in Fig. 8. This plot shows that $\text{Im}(Z_2) > \text{Re}(Z_2)$ for frequencies less than 115 Hz where a surface wave is expected according to Eq. (7). This result is consistent with the measured power spectra

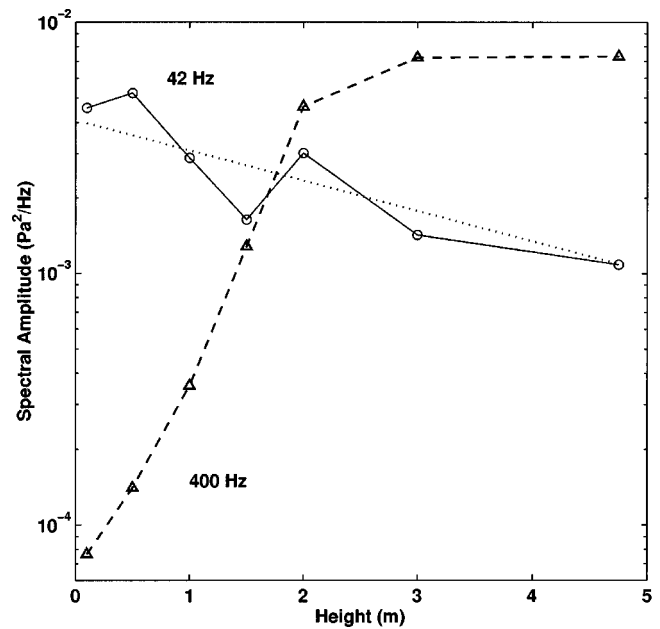


FIG. 7. The spectral amplitude as a function of height for the measured waveforms for Experiment 2, at 42 Hz (circles and solid line) and at 400 Hz (triangles and dashed line). The dotted line shows the attenuation trend for $\alpha = -0.28$ in Eq. (13) and in Fig. 4.

shown in Fig. 6 if we identify the low frequency portion of the spectra (with a peak at about 42 Hz) with the acoustic surface wave. The surface wave phase velocity and attenuation calculated from the impedance using Eqs. (9) and (10) are also shown in Fig. 8. The surface wave velocity is less

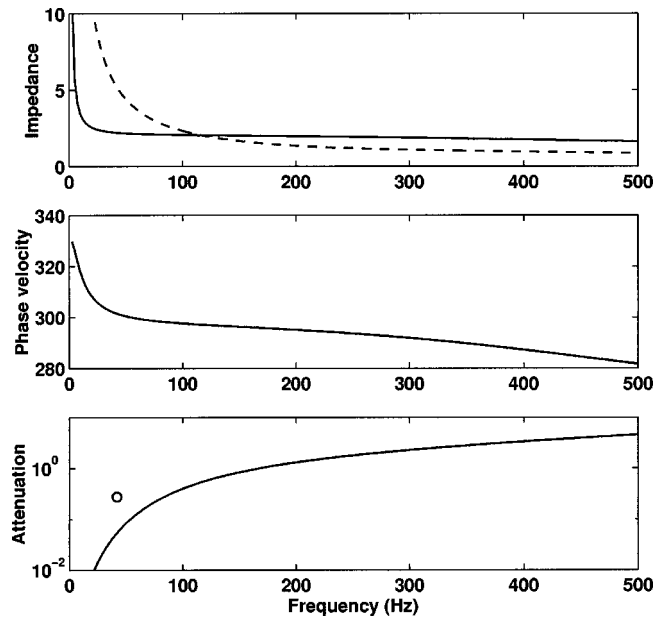


FIG. 8. Acoustic surface wave properties for Experiment 2. The top panel shows the surface impedance as predicted using Attenborough’s ground impedance model and the parameters determined from the waveform inversion analysis. The real part of the impedance is given by the solid line, while the dashed line shows the absolute value of the imaginary part. The phase velocity (m s^{-1}) and attenuation (m^{-1}) are shown in the center and bottom panels, respectively. These values were calculated using Eqs. (9) and (10) and the impedance shown in the top panel. Note that the surface wave is only expected to exist for frequencies below 115 Hz, based on Eq. (7). The circle plotted in the bottom panel is the attenuation measured in Fig. 4.

than the speed of sound in air, as expected and in agreement with the identification of the low frequency tail that arrives after the direct and reflected waves as the acoustic surface wave. The measured attenuation of 0.28 m^{-1} (from Fig. 4) is plotted at the peak frequency, 42 Hz, of the surface wave spectrum, and agrees with the theoretical attenuation, given the accuracy of the attenuation measurement as discussed above.

V. CONCLUSIONS

Acoustic surface waves have been experimentally observed propagating above a snow cover. The similarity between the observed and theoretical waveform shapes that were calculated using an explicit surface wave expression [Eq. (12)] is especially strong evidence that the identification of the observed waveforms as acoustic surface waves is correct. The acoustic surface wave for a 0.21-m-thick snow cover was observed to decay exponentially with height above the surface, with a decay constant of 0.28 m^{-1} . The results also indicate that the details of the layering within the snow are relatively unimportant, at least for these particular snow covers. Surface waves were not observed over grass or bare frozen ground, also in agreement with theoretical expectations.

ACKNOWLEDGMENTS

I thank Gilles Daigle for useful discussions at the Fourth International Symposium on Long Range Sound Propagation that led to these experiments, and for comments on early versions of the manuscript. Many of my coworkers assisted with these experiments; I would especially like to thank Steve Decato for serving as the shooter and Nancy Greeley for providing the meteorological data. They also performed the snow characterization and provided additional assistance with the experiments. Thanks also goes to Steve Arcone and two anonymous reviewers for useful comments, and to the Associate Editor Lou Sutherland for many suggested improvements. This work is supported by the Directorate of Research and Development, U.S. Army Corps of Engineers.

¹L. M. Brekhovskikh, "Surface waves in acoustics," *Sov. Phys. Acoust.* **5**, 3–12 (1959).
²R. J. Donato, "Propagation of a spherical wave near a plane boundary with complex impedance," *J. Acoust. Soc. Am.* **60**, 34–39 (1976).
³S. I. Thomasson, "Sound propagation above a layer with large refractive index," *J. Acoust. Soc. Am.* **61**, 659–674 (1977).
⁴A. R. Wenzel, "Propagation of waves along an impedance boundary," *J. Acoust. Soc. Am.* **55**, 956–963 (1974).
⁵J. Tizianel, J.-F. Allard, W. Lauriks, and L. Kelders, "Experimental localization of a pole of the reflection coefficient of a porous layer," *J. Sound Vib.* **202**, 600–604 (1997).
⁶J. Tizianel, J. F. Allard, and B. Brouard, "Surface waves above honeycombs," *J. Acoust. Soc. Am.* **104**, 2525–2528 (1998).
⁷W. Lauriks, L. Kelders, and J.-F. Allard, "Surface waves and leaky waves above a porous layer," *Wave Motion* **28**, 59–67 (1998).
⁸W. Lauriks, L. Kelders, and J. F. Allard, "Surface waves above gratings having a triangular profile," *Ultrasonics* **36**, 865–871 (1998).
⁹L. Kelders, W. Lauriks, and J. F. Allard, "Surface waves above thin porous layers saturated by air at ultrasonic frequencies," *J. Acoust. Soc. Am.* **104**, 882–889 (1998).
¹⁰L. Kelders, J. F. Allard, and W. Lauriks, "Ultrasonic surface waves above

rectangular-groove gratings," *J. Acoust. Soc. Am.* **103**, 2730–2733 (1998).
¹¹J. F. Allard, L. Kelders, and W. Lauriks, "Ultrasonic surface waves above a doubly periodic grating," *J. Acoust. Soc. Am.* **105**, 2528–2531 (1999).
¹²G. Daigle and T. Embleton, "Air-ground interface: surface waves, surface impedance and acoustic-to-seismic coupling coefficient," *Proceedings of the 4th International Symposium on Long-Range Sound Propagation*, NASA CP 3101, NASA, Hampton, VA, 17 May 1990, pp. 27–40.
¹³G. A. Daigle, "Role of surface waves in outdoor noise propagation," *1991 International Conference on Noise Control Engineering (Inter-Noise 91)*, Noise Control Foundation, Poughkeepsie, NY, Sydney, Australia, 2–4 December 1991.
¹⁴G. A. Daigle, M. R. Stinson, and D. I. Havelock, "Experiments on surface waves over a model impedance plane using acoustical pulses," *J. Acoust. Soc. Am.* **99**, 1993–2005 (1996).
¹⁵R. J. Donato, "Model experiments on surface waves," *J. Acoust. Soc. Am.* **63**, 700–703 (1978).
¹⁶M. R. Stinson, G. A. Daigle, and D. I. Havelock, "The formation of surface waves over a model surface," *Proceedings of the 5th International Symposium on Long Range Sound Propagation*, Milton Keynes, England, 24–26 May 1992, pp. 17–28.
¹⁷K. B. Rasmussen, "Sound-propagation over grass covered ground," *J. Sound Vib.* **78**, 247–255 (1981).
¹⁸J. Nicolas, J.-L. Berry, and G. A. Daigle, "Propagation of sound above a finite layer of snow," *J. Acoust. Soc. Am.* **77**, 67–73 (1985).
¹⁹C. G. Don and A. J. Cramond, "Impulse propagation in a neutral atmosphere," *J. Acoust. Soc. Am.* **81**, 1341–1349 (1987).
²⁰R. Raspet, H. E. Bass, and J. Ezell, "Effect of finite ground impedance on the propagation of acoustic pulses," *J. Acoust. Soc. Am.* **74**, 267–274 (1983).
²¹R. Raspet, J. Ezell, and H. E. Bass, "Additional comments on and erratum for 'Effect of finite ground impedance on the propagation of acoustic pulses' [*J. Acoust. Soc. Am.* **74**, 267–274 (1983)]," *J. Acoust. Soc. Am.* **77**, 1955–1958 (1985).
²²R. Raspet and G. E. Baird, "The acoustic surface wave above a complex impedance ground surface," *J. Acoust. Soc. Am.* **85**, 638–640 (1989).
²³G. A. Daigle (personal communication, 1990).
²⁴K. Attenborough, "Review of ground effects on outdoor sound propagation from continuous broadband sources," *Appl. Acoust.* **24**, 289–319 (1988).
²⁵K. Aki and P. G. Richards, *Quantitative Seismology: Theory and Methods* (Freeman, San Francisco, 1980), Vol. 1, p. 155.
²⁶W. M. Ewing, W. S. Jardetzky, and F. Press, *Elastic Waves in Layered Media* (McGraw-Hill, New York, 1957).
²⁷P. M. Morse and K. U. Ingard, *Theoretical Acoustics* (Princeton University Press, Princeton, NJ, 1968), p. 927.
²⁸J. A. Stratton, *Electromagnetic Theory* (McGraw-Hill, New York, 1941).
²⁹C. F. Chien and W. W. Soroka, "Sound propagation along an impedance plane," *J. Sound Vib.* **43**, 9–20 (1975).
³⁰I. Rudnick, "Propagation of an acoustic wave along a boundary," *J. Acoust. Soc. Am.* **19**, 348–356 (1947).
³¹K. U. Ingard, "On the reflection of a spherical wave from an infinite plane," *J. Acoust. Soc. Am.* **23**, 329–335 (1951).
³²K. Attenborough, S. I. Hayek, and J. M. Lawther, "Propagation of sound above a porous half-space," *J. Acoust. Soc. Am.* **68**, 1493–1501 (1980).
³³C. F. Chien and W. W. Soroka, "A note on the calculation of sound propagation along an impedance surface," *J. Sound Vib.* **69**, 340–343 (1980).
³⁴D. G. Albert, "Acoustic waveform inversion with application to seasonal snow covers," *J. Acoust. Soc. Am.* **109**, 91–101 (2001).
³⁵J. M. Sabatier, R. Raspet, and C. K. Frederickson, "An improved procedure for the determination of ground parameters using level difference measurements," *J. Acoust. Soc. Am.* **94**, 396–399 (1993).
³⁶K. Attenborough, "Acoustical impedance models for outdoor ground surfaces," *J. Sound Vib.* **99**, 521–544 (1985).
³⁷D. G. Albert, "Observations of acoustic surface waves propagating above a snow cover," in Ref. 16, 1992, pp. 10–16.
³⁸D. J. Thomson, "Spectrum estimation and harmonic analysis," *Proc. IEEE* **70**, 1055–1096 (1982).
³⁹D. G. Albert and J. A. Orcutt, "Acoustic pulse propagation above grassland and snow: Comparison of theoretical and experimental waveforms," *J. Acoust. Soc. Am.* **87**, 93–100 (1990).